

Comparative Study of the Performance of Packed Beds Using Different Types of Thermal Storage Materials

Aicha Eddemani^{1*} , Hayat El Baamrani², Ahmed Aharoune³, Lahcen Bouriden⁴,
Ahmed Ihlal⁵.

^{1,2,3,4}Thermodynamic and Energetics Laboratory, Physics Department, Faculty of Sciences,
University of Ibn Zohr, Agadir, Morocco.

⁵Materials and Renewable Energies Laboratory, Physics Department, Faculty of Sciences,
University of Ibn Zohr, Agadir, Morocco.

E-mail: ¹eddemani.aicha@gmail.com.

SPECIAL ISSUE ON:

The 2024 1st International Conference
on Materials Sciences and Mechatronics
for Sustainable Energy and the Environment
October 1-3, 2024 at Béni-Mellal, Morocco

ABSTRACT

In packed bed thermal energy storage (PBTES) systems, the selection of a suitable storage material as packing material depends on several factors, including specific heat capacity, desired temperature range, heat transfer properties, thermal stability, cost-effectiveness, and availability. This work offers a comparative analysis of various thermal storage materials, providing valuable insights into their performance and suitability for energy storage applications. A numerical method, subsequently confirmed by experimental results, was used to analyze the performance of the studied packed beds, taking into account the thermo-physical characteristics of the different storage materials.

KEYWORDS

Thermal storage; Packed bed;
Solar energy; CFD analysis; SHS
materials.

Numerical simulations were carried out over the charging and discharging periods. The findings indicate that the thermal properties of the materials under investigation have a significant impact on the stratification and efficiency of the system. Among the materials evaluated, quartzite emerges as the most promising Sensible Heat Storage (SHS) material for PBTES systems, offering an optimal balance of thermal performance and cost-effectiveness, making it a highly suitable choice for large-scale thermal energy storage applications.

*Corresponding author.



دراسة مقارنة لأداء الأسرة المعبأة باستخدام أنواع مختلفة من مواد تخزين الحرارة

عائشة الدماني ، حياة البعمراني، أحمد أهروان، لحسن بويردن، أحمد إهلال .

ملخص: في أنظمة تخزين الطاقة الحرارية ذات السريان المعبأ (PBTES)، يعتمد اختيار مادة التخزين المناسبة كمادة تعبئة على عدة عوامل، بما في ذلك السعة الحرارية النوعية، نطاق درجات الحرارة المطلوب، خصائص انتقال الحرارة، الاستقرار الحراري، التكلفة، والتوافر. يقدم هذا العمل تحليلاً مقارناً لمواد تخزين حرارية مختلفة، مما يوفر رؤى قيمة حول أدائها ومدى ملاءمتها لتطبيقات تخزين الطاقة. تم استخدام طريقة عددية، تم تأكيدها لاحقاً بنتائج تجريبية، لتحليل أداء الأسرة المعبأة التي تمت دراستها مع مراعاة الخصائص الفيزيائية الحرارية للمواد المختلفة. تم إجراء المحاكاة العددية خلال فترتي الشحن والتفريغ. تشير النتائج إلى أن الخصائص الحرارية للمواد قيد الدراسة لها تأثير كبير على التدرج الحراري وكفاءة النظام. من بين المواد التي تم تقييمها، يظهر الكوارتزيت كأفضل مادة تخزين حراري معتمدة على الحرارة الحسّية (SHS) لأنظمة PBTES، حيث يوفر توازناً مثالياً بين الأداء الحراري والتكلفة، مما يجعله خياراً مناسباً للغاية لتطبيقات تخزين الطاقة الحرارية على نطاق واسع.

الكلمات المفتاحية: - التخزين الحراري، السريان المعبأ، الطاقة الشمسية، تحليل ديناميكا الموائع الحسابية (CFD)، مواد تخزين الحرارة الحسّية (SHS).

1. INTRODUCTION

Concentrated solar power (CSP) plants offer a promising solution for harnessing the potential of solar energy. However, to address the intermittent nature of solar energy, it is crucial to integrate thermal storage into solar power plants in order to enhance their reliability, efficiency, and economic feasibility, as well as ensure a continuous supply of clean energy to meet the increasing demands [1]. Thermal Energy Storage (TES) systems utilize different types of storage materials based on their thermal properties and the mechanisms by which they store and release energy. The primary types of storage materials can be classified into three main categories: Sensible Heat Storage (SHS), Latent Heat Storage (LHS), and Thermochemical Storage (TCS). SHS materials accumulate energy by increasing their temperature without undergoing a phase change [2]. LHS materials, commonly known as Phase Change Materials (PCMs), store energy through phase transitions [3]. They offer near-isothermal operation but are often limited by lower thermal conductivity and potential issues with cycling stability [4]. TCS materials store energy through reversible chemical reactions, providing even greater energy density but often require careful management of factors such as temperature and pressure, adding complexity to their implementation and operation [4].

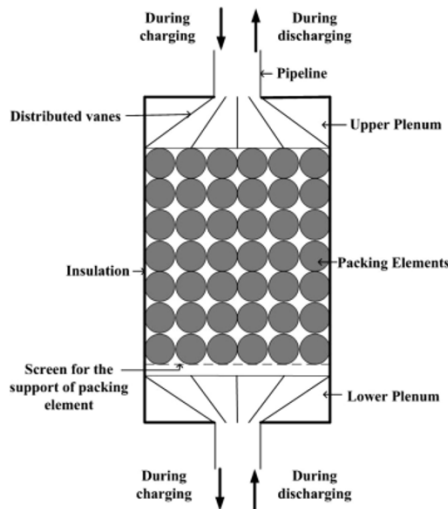


Figure 1: Representation of a PBTES system [6].

Nevertheless, among the three categories, SHS materials offer significant benefits such as simplicity

in their operation, lower costs, long-lasting durability, and flexibility in their applications, making them an easier and more cost-effective option for many TES systems [5].

A PBTES system is a TES device that employs a bed of solid materials. These materials act as the storage medium, absorbing and retaining heat, which can be transferred back to a working fluid, such as air, during the discharge process when the stored energy is required for recovery or use (Figure 1). These systems are increasingly recognized for their simplicity and high efficiency when incorporated into solar power plants [6].

Selecting the most appropriate material for the PBTES system involves considering several key criteria. These criteria ensure the material will provide efficient, reliable, and cost-effective energy storage. The key factors to consider when choosing thermal storage materials are [7]:

- Cost- effectiveness and availability;
- Positive environmental effect;
- Large thermal storage capacity;
- Usability in high-temperature conditions;
- High resistance to thermal cycling;
- Compatibility with heat-transfer fluids;
- Easy Implementation.

Based on specific requirements such as cost and temperature range, various materials can be employed as storage media in the PBTES system. Sensible storage materials are less expensive than latent and thermochemical materials and enable the achievement of high temperatures without deterioration [8]. A variety of SHS materials can be utilized in PBTES systems, depending on the temperature range and specific application: natural rocks, ceramic materials, concrete and metallic materials [8][9].

The limited studies in the literature regarding the behavior of the thermocline zone during the charging and discharging phases for various storage materials underscore the significance of the present work. This gap in research highlights the necessity for a comprehensive examination of how different materials interact within the thermocline zone, particularly as it pertains to their thermal performance and efficiency in PBTES systems. The SHS materials examined comprise alumina, quartzite, cast steel, and ceramic. By addressing this critical area, the current study aims to identify the most effective options that can improve thermal efficiency and enhance system performance in PBTES applications. The thermal properties of the various storage materials are listed in Table 1.

Table 1. Thermal properties of the storage materials examined [8].

Material	ρ [kg/m ³]	c_p [kg/m ³]	ρc_p [kJ/m ³ K]	k [W/mK]	Cost [€/t]
Alumina	3960	800	3168	18	5000
Ceramic	3500	866	3031	1.35	4500
Cast steel	7800	600	4680	40	4430
Quartzite	2570	1185	3046	3.5	0.5

2. MODELING

This work is conducted using ANSYS-Fluent, a powerful computational fluid dynamics (CFD) software. A validated unsteady two-phase numerical model [10] was employed to assess the effectiveness of the PBTES system. The geometry considered in the numerical analysis is two-dimensional axisymmetric cylindrical unit with an inner diameter of 0.148 m and a height of 1.2 m. It is discretized into a computational mesh of quadrilateral type, ensuring a finer resolution near boundaries and interfaces to accurately capture temperature gradients and flow patterns.

The simulation incorporated both solid and fluid phases of the storage media. The air serves as the fluid phase, functioning as the heat transfer fluid, while the solid phase represents the storage materials. The highest temperature of 823K is associated with the fluid inlet during the charging phase, whereas the minimum temperature of 293K corresponds to the fluid inlet during the discharging period.

This study makes several key assumptions to simplify the analysis of the PBTES system: air is treated as a perfect gas, fluid flow is laminar, and the temperature within each rock is uniformly distributed, a result of the Biot number (Bi) being below 1. The thermal properties of the fluid are considered to be temperature-dependent, with no internal heat generation present. Additionally, heat transfer by radiation is neglected, focusing the analysis on conduction and convection processes.

The two-phase model addresses heat transfer in packed beds by independently analyzing the solid and fluid phases. This method entails formulating and solving distinct energy equations for each phase [8]. As a result, the model provides a more thorough and accurate representation of heat transfer mechanisms, allowing for the assessment of interactions and temperature variations between the solid and fluid elements in the system [8]. The energy equations for the fluid and solid phases are represented by Equations (1) and (2), respectively.

$$\frac{\partial}{\partial t}(\varepsilon \rho_f c_p T_f) + \nabla(\bar{v} \rho_f c_p T_f) = \nabla(\varepsilon k_f \nabla T_f) + h_{fs} A (T_s - T_f) + h_{fw} A_w (T_w - T_f) \quad (1)$$

$$\frac{\partial}{\partial t}((1-\varepsilon) \rho_s c_s T_s) = \nabla((1-\varepsilon) k_s \nabla T_s) + h_{fs} A (T_s - T_f) \quad (2)$$

T_f and T_s denote the temperatures of the fluid and solid, respectively. The variable ε represents the void fraction within the packed bed. The convective heat transfer coefficients are denoted as h_{fs} (W/m² K) for the interaction between the fluid and the solid, and h_{fw} (W/m² K) for the interaction between the fluid and the wall. A (m²) indicates the surface area, while T_w (K) represents the temperature of the wall.

The dimensionless temperature θ in a packed bed provides a dimensionless metric for comparing temperatures across various conditions within the range of minimum and maximum temperatures:

$$\theta = \frac{T - T_{min}}{T - T_{max}} \quad (3)$$

σ represents the ratio of the amount of energy stored (e_{st}) during the charging process to the highest energy storage capacity of the tank (e_{st}^{max}).

$$\sigma = \frac{e_{st}}{e_{st}^{max}} \quad (4)$$

The overall efficiency (η) of a PBTES system can be defined as the ratio of the useful energy recovered from the system during the discharge phase to the energy supplied to the system during the charge process. It is expressed as:

$$\eta = \frac{e_{out}}{e_{in}} \quad (5)$$

e_{in} denotes the energy supplied during the charging phase.

$$e_{in} = \int_0^{t_{charge}} \phi_{in}(t) dt \quad (6)$$

$\phi_{in}(t)$ is the rate of heat input as a function of time during the charging period.

e_{out} indicates the useful energy retrieved during the discharge phase.

$$e_{out} = \int_0^{t_{discharge}} \phi_{out}(t) dt \quad (7)$$

$\phi_{out}(t)$ is the rate of heat output as a function of time during the discharge period.

Reference [11] provides a detailed description of the experimental investigation conducted to confirm the validity of the numerical model. The system features a cylindrical container filled with rock particles with an equivalent spherical diameter of 0.02 m, utilizing air as the working fluid [11]. The tank dimensions include a height of 1.2 m and a diameter of 0.148 m. Air flows through the system at a mass flow rate of 0.225 kg/m²s [11].

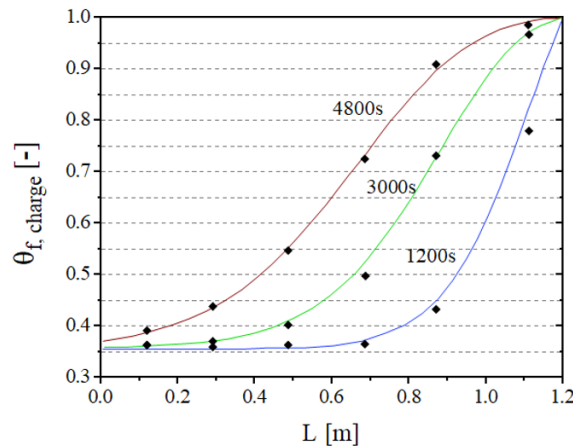


Figure 2: Dimensionless numerical (line) and experimentally measured (symbol) temperatures.

The comparison between the experimental data and numerical outcomes is illustrated in Figure (2). The findings indicate that the numerical results closely match the experimental values, demonstrating a high level of agreement between the two sets of data.

3. RESULTS AND DISCUSSION

Figure 3 presents the thermal capacity and cost of each storage material. It indicates that cast steel possesses the highest thermal storage capacity, whereas alumina, ceramic, and quartzite have almost identical thermal capacities. However, there is a significant difference in cost: quartzite (0.5 €/t) is substantially less expensive compared to alumina and ceramic.

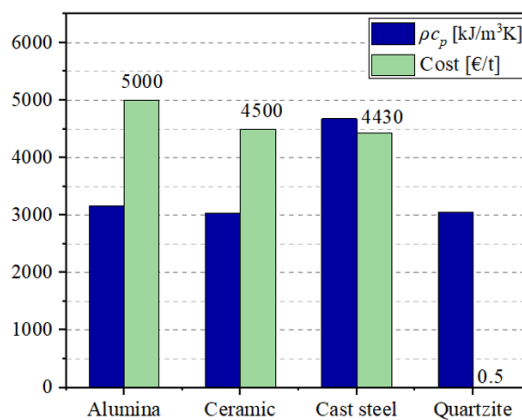


Figure 3: Thermal capacity and cost of different storage materials.

Figure 4 shows the dimensionless temperature profiles of storage materials at the end of the charging phase. It indicates that the temperature changes follow similar trends; however, the behavior of the thermozone and its thickness exhibited different variations. The temperatures of the

ceramic and quartzite are close throughout the tank, reaching a maximum temperature ($\theta=1$) at a height of 1.2 m. However, the temperature of the bed filled with cast steel is notably lower than that of the other beds. This can be attributed to its high thermal capacity, which requires a longer charging time as it can absorb and store more energy before reaching its maximum temperature. Additionally, the exceptionally high thermal conductivity of cast steel enables heat to diffuse more rapidly between the solid particles, resulting in a faster redistribution of heat throughout the material. While this promotes a more uniform temperature distribution, it also means that the overall temperature rise is slower compared to materials with lower thermal conductivity.

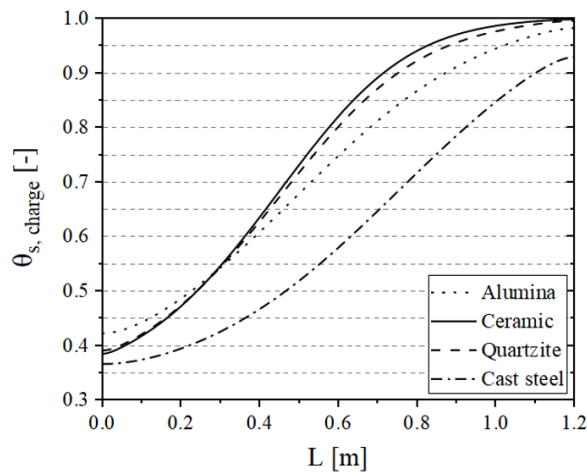


Figure 4: Dimensionless temperature profiles of storage materials at the end the charging phase.

Figure 5 shows the evolution of the average dimensionless temperature of storage materials over 2h of charging period. It shows that a linear increase in temperature for all four thermal storage materials. Notably, the temperatures of ceramic and quartzite are nearly indistinguishable, both reaching an average dimensionless temperature of 0.75 by the end of the charging phase. In contrast, alumina reaches an average dimensionless temperature of 0.72, while cast steel attains a lower dimensionless temperature of 0.61.

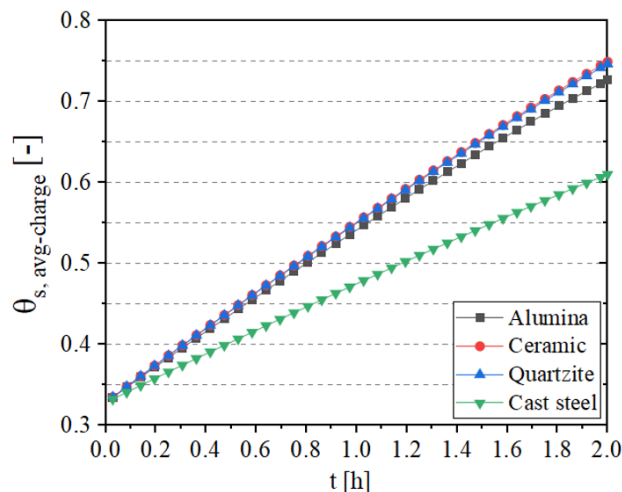


Figure 5: Evolution of the dimensionless average temperature of storage materials during the charge cycle.

The axial dimensionless temperature at the end of the discharge is shown in Figure 6. As can be seen, the ceramic and quartzite temperatures are higher in the upper 0.13m zone. However, the results are reversed for the rest of the tank. The cast steel temperature is higher, and the ceramic temperature is lower. The temperature decline observed at the top of the cast steel and alumina

beds can be attributed to their high thermal conductivity, which facilitates a more efficient and rapid heat transfer throughout the packed bed. This property enables these materials to rapidly distribute heat, causing the upper sections to cool more quickly while maintaining high temperatures in the lower parts of the tank.

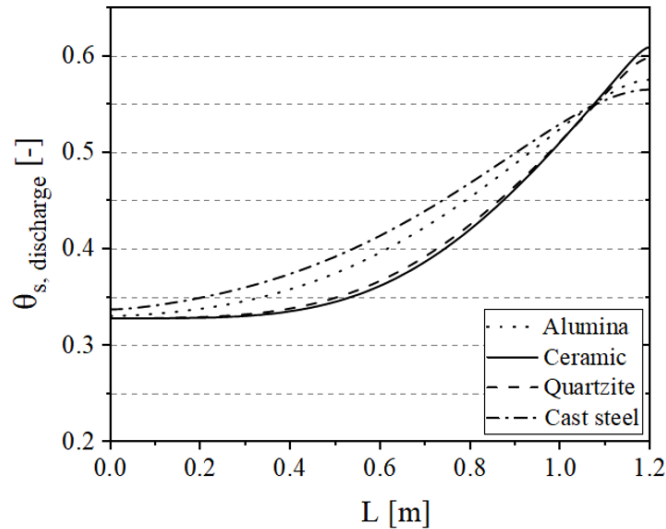


Figure 6: Dimensionless temperature profiles of storage materials during discharge.

Figure 7 shows that during the discharge phase, the dimensionless fluid outlet temperature from the ceramic bed is the highest, closely matching that of quartzite. Furthermore, at the start of the discharge, the fluid outlet temperatures from the ceramic and quartzite beds are recorded at 0.98 and 0.97, respectively, both approaching the maximum temperature. In contrast, the outlet temperatures from the alumina and cast steel beds are the lowest compared to other beds.

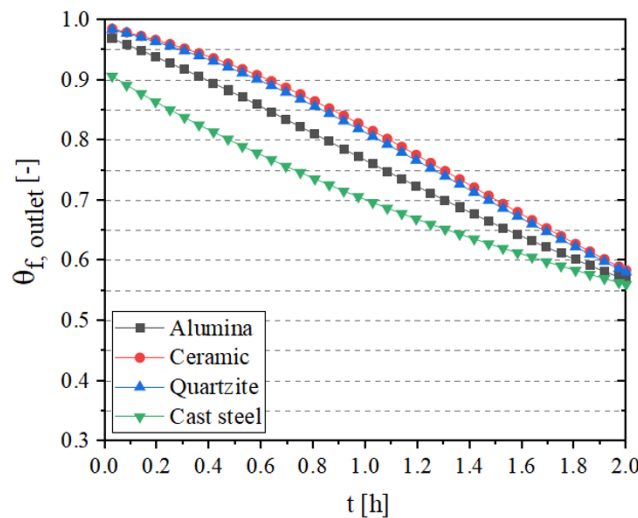


Figure 7: Dimensionless fluid outlet temperature throughout the discharge period.

The results presented in Figure 7 directly impact the efficiency of the storage system, as illustrated in Figure 8. The ceramic bed achieved an efficiency of 72% and a capacity ratio of 63%. The efficiency and capacity ratio of quartzite are 71% and 62%, respectively, which are comparable to those of ceramic. However, in terms of cost, quartzite is more cost-effective, being 9,000 times less expensive than ceramic (as shown in Figure 3). The alumina bed achieved an efficiency of 67% with a capacity ratio of 59%. On the other hand, the efficiency of cast steel at the end of

the first charge-discharge cycle was limited to 49%, which is due to its very high density and moderate specific heat capacity.

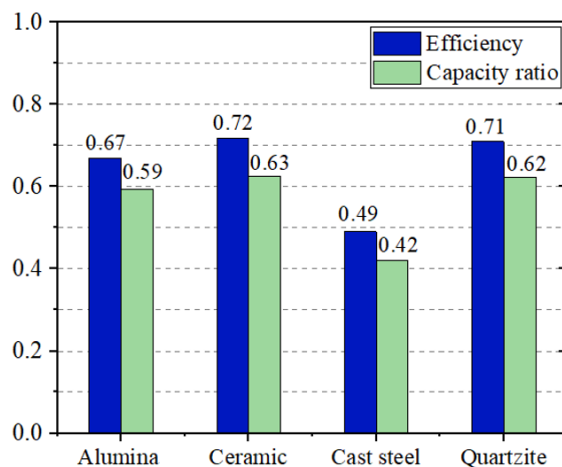


Figure 8: Performance of packed beds containing various storage materials.

4. CONCLUSION

A computational model has been developed and validated to simulate the thermal behavior of different materials, namely ceramic, quartzite, alumina, and cast steel. Numerical simulations were performed for both the charging and discharging phases. The simulation outcomes revealed that ceramic and quartzite outperformed alumina and cast steel in terms of thermal efficiency. However, despite ceramic and quartzite exhibited similar thermal performance, quartzite emerged as the more cost-effective option, providing a significant economic advantage. In summary, the findings position quartzite as the most promising sensible heat storage material for PBTES systems, combining superior thermal properties with low cost, thereby making it an ideal choice for large-scale TES applications.

Authors contribution: Author Contributions: All authors have made a substantial, direct, and intellectual contribution to the work and approved it for publication.

Funding: There is no funding for the article.

Data Availability Statement: Data Availability Statement: Not applicable.

Conflicts of Interest: The authors declare that they have no conflict of interest.

Acknowledgements: The authors would like to thank all individuals and organizations who contributed to this work. We are especially grateful to colleagues and collaborators for their constructive feedback and insightful discussions. We also extend our appreciation to the supporting staff and institutions for providing the resources and facilities that made this study possible.

REFERENCES

- [1] J. Mitali, S. Dhinakaran, and A.A. Mohamad, "Energy storage systems: a review," *Energy Storage Sav.*, vol. 1, p. 166–216, 2022. <https://doi.org/10.1016/j.enss.2022.07.002>
- [2] R. Mabrouk, H. Naji, A. C. Benim, and H. Dhahri, "A State of the Art Review on Sensible and Latent Heat," *Appl. Sci.*, vol. 12, p. 6995, 2022. <https://doi.org/10.3390/app12146995>

- [3] L. Gao, Gegentana, J. Bai, B. Sun, D. Che, S. Li, "Parametric analysis of a packed bed thermal storage device with phase change material capsules in a solar heating system application," *Build. Simul.*, vol. 14, p. 523–533, 2021. <https://doi.org/10.1007/s12273-020-0686-2>
- [4] M. Tawalbeh, H. A. Khan, A. Al-Othman, F. Almomani, and S. Ajith, "A comprehensive review on the recent advances in materials for thermal energy storage applications," *Int. J. Thermofluids*, vol. 18, p. 100326, 2023. <https://doi.org/10.1016/j.ijft.2023.100326>
- [5] B. Koçak, A. I. Fernandez, and H. Paksoy, "Review on sensible thermal energy storage for industrial solar applications and sustainability aspects," *Sol. Energy*, vol. 209, p. 135-169, 2020. <https://doi.org/10.1016/j.solener.2020.08.081>
- [6] A. Gautam, and R.P. Saini, "A review on technical, applications and economic aspect of packed bed solar thermal energy storage system," *J. Energy Storage*, vol. 27, p. 101046, 2020. <https://doi.org/10.1016/j.est.2019.101046>
- [7] A. Meffre, "Matériaux de stockage thermique haute température issus de la valorisation de matières premières secondaires inorganiques," Ph.D. thesis, Université de Perpignan Via Domitia, 2013.
- [8] I. C. Vásquez, E. Cortés, J. García, V. Segovia, A. Caroca, C. Sarmiento, R. Barraza, and J. M. Cardemil, "Review on modeling approaches for packed-bed thermal storage systems," *Renew. Sustain. Energy Rev.* vol. 143, p. 110902, 2021. <https://doi.org/10.1016/j.rser.2021.110902>
- [9] P. R. Olivkar, V. P. Katekar, S. S. Deshmukh, S. V. Palatkar, "Effect of sensible heat storage materials on the thermal performance of solar air heaters: State-of-the-art," review. *Renew. Sustain. Energy Rev.*, vol. 157, p. 112085, 2022. <https://doi.org/10.1016/j.rser.2022.112085>
- [10] A. Eddemani, L. Bammou, R. Tiskatine, A. Aharoune, L. Bouirden, and A. Ihlal, "Evaluation of the thermal performance of the air-rock bed solar energy storage system," *Int. J. Ambient Energy*, vol. 42, p. 1699–1707, 2019. <https://doi.org/10.1080/01430750.2019.1614982>
- [11] M. Hänchen, S. Brückner and A. Steinfeld, "High-temperature thermal storage using a packed bed of rocks – heat transfer analysis and experimental validation". *Appl. Therm. Eng.* vol. 31, p. 1798–1806, 2011. <https://doi.org/10.1016/j.applthermaleng.2010.10.034>